

## Supplementary materials

# The interplay between GSK3 $\beta$ and tau Ser262 phosphorylation during the progression of tau pathology

Liqing Song<sup>1</sup>, Daniel E Oseid<sup>2</sup>, Evan A. Wells<sup>1</sup>, Anne Skaja Robinson<sup>1, \*</sup>

<sup>1</sup> Department of Chemical Engineering, Carnegie Mellon University, Pittsburgh, PA, 15213, USA

<sup>2</sup> Tulane Brain Institute, Tulane University, New Orleans, LA, 70118, USA

\* Correspondence: anne.robinson@cmu.edu; Tel.: (+1) 412-268-7673 (A.S.R.)

## Supplementary Table S1. A list of antibodies

Primary Antibody	Origin/ Isotype	Supplier/ Cat#	Secondary antibody
pS199	Rabbit IgG	Life Technologies, 44734G	Alexa Fluor® 488 goat anti-Rabbit IgG H&L (Abcam, ab150077)
pT231	Rabbit IgG	Abcam, ab151559	Alexa Fluor® 488 goat anti-Rabbit IgG H&L (Abcam, ab150077)
HT7	Rabbit IgG	Life Technologies, MN1000	Alexa Fluor® 488 goat anti-Rabbit IgG H&L (Abcam, ab150077)
T22	Rabbit IgG	Millipore Sigma, ABN454	Alexa Fluor® 488 goat anti-Rabbit IgG H&L (Abcam, ab150077)
Tau-5	Mouse IgG1	Life Technologies, MA512808	Alexa Fluor® 594 goat anti-Mouse IgG1 (Invitrogen, A-21125)
$\beta$ -tubulin	Rabbit IgG	Cell Signaling, 3700T	Alexa Fluor® 488 goat anti-Rabbit IgG H&L (Abcam, ab150077)
AT8	Mouse IgG1	Life Technologies, MN1020	Alexa Fluor® 594 goat anti-Mouse IgG1 (Invitrogen, A-21125)
77G7	Mouse IgG1	BioLegend, SIG-39405	Alexa Fluor® 594 goat anti-Mouse IgG1 (Invitrogen, A-21125)
6HCLC	Rabbit IgG	Life Technologies, 710080	Alexa Fluor® 488 goat anti-Rabbit IgG H&L (Abcam, ab150077)
MAP2	Mouse IgG1	Millipore Sigma, M1406	Alexa Fluor® 594 goat anti-Mouse IgG1 (Invitrogen, A-21125)
$\beta$ -actin	Mouse IgG	Cell Signaling, 8H10D10	Alexa Fluor® 488 goat anti-Mouse (H+L) (Invitrogen, A-11029)
Syntenin-1	Rabbit IgG	Abcam, ab133267	Alexa Fluor® 488 goat anti-Rabbit IgG H&L (Abcam, ab150077)

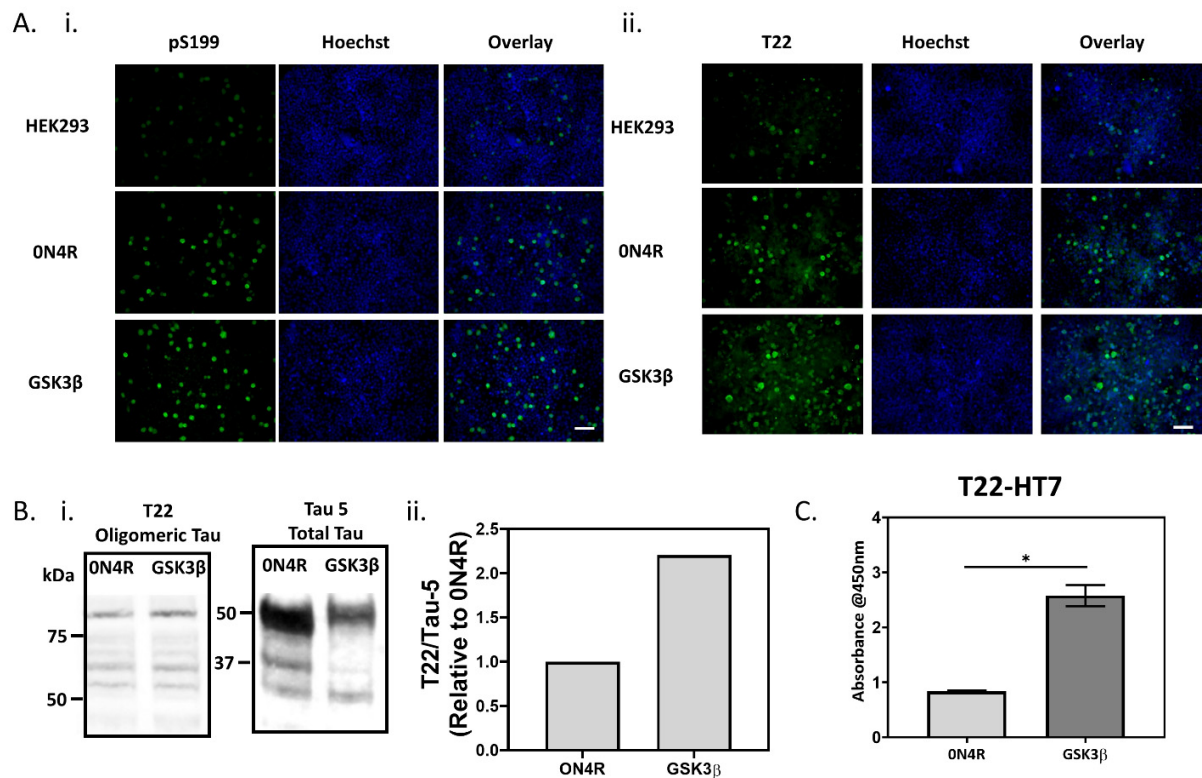


**Figure S1. The biochemical characterization of HEK293 cells expressing wild type 0N4R and GSK3β constructs.** Representative fluorescent images of tau markers, including pS199 (Green)/Hoechst (Blue) (A.i.) and T22(Green)/Hoechst (Blue) (A.ii.) for HEK293 cells 3 days post-transfection. Scale bar = 100 μm. Cell lysates from two groups were analyzed by immunoblotting (B.i.) against oligomeric tau antibody, T22, and the total tau antibody, Tau-5, followed by quantitation (B.ii.) of T22/Tau-5 ratios from a representative western blot experiment. C. The oligomeric and total tau were measured by sandwich ELISA using T22 and human tau antibody, HT7, respectively. (\* represents p<0.05 for 0N4R compared with GSK3β (n=3)).

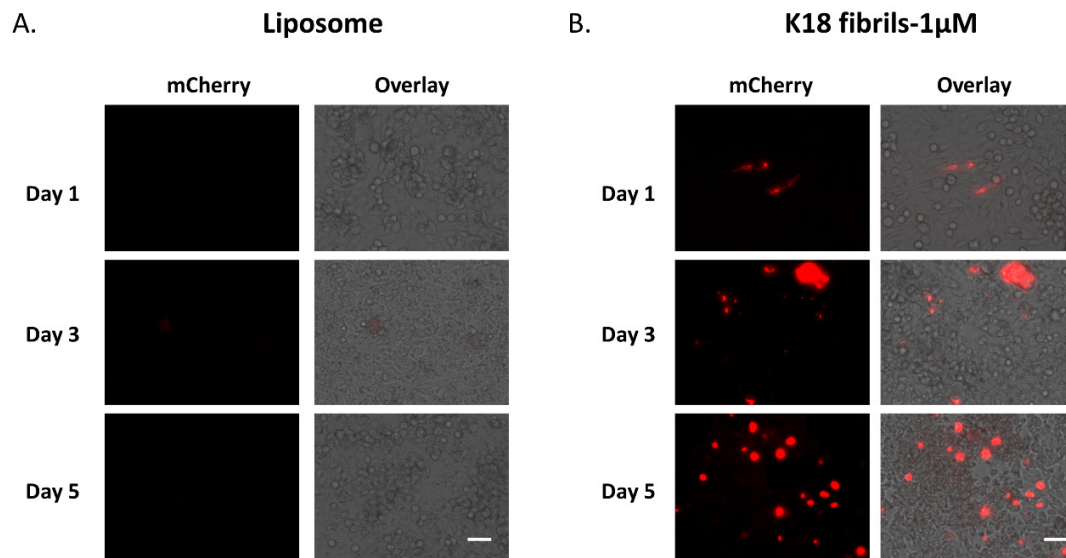


**Figure S2. The tau seeding activity of tau-tau sfCherry biosensor CHO K1 cells induced by 1 $\mu$ M K18 fibrils.** Fluorescence microscopy images of tau-tau sfCherry biosensor cells treated with 1  $\mu$ M of K18 tau fibrils for 5 days. Liposome only group showed no red signals. The scale bar denotes 100  $\mu$ m.

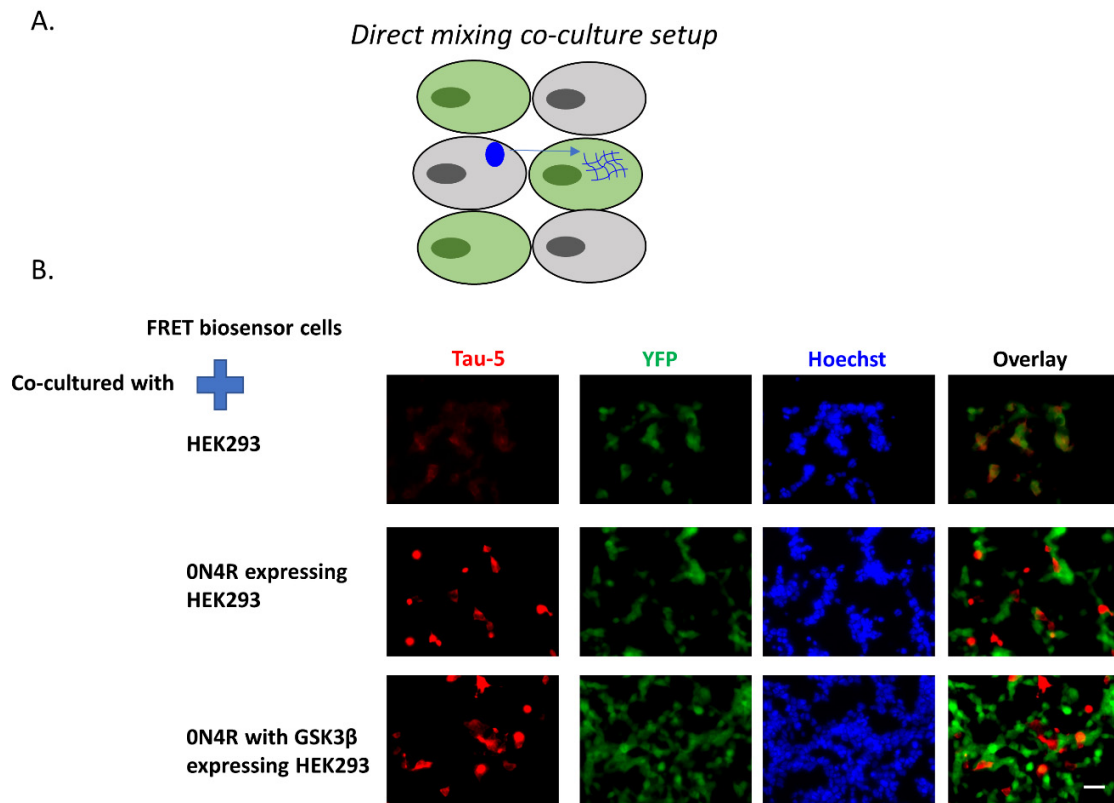


**Figure S3 Direct mixing tau-expressing HEK293 cells with FRET tau biosensor cells.** **A.** The schematic illustration of the direct mixing co-culture setup to investigate transcellular tau propagation. **B.** Cells were immunostained against Tau-5 (Red) after three days of co-culturing. The scale bar denotes 100  $\mu\text{m}$ . Transfecting HEK293 cells have indeed increased the amount of Tau-5+ cell population in both ON4R and ON4R with GSK3 $\beta$ -expressing HEK293 cells. However, there were no visible tau aggregates formed in tau FRET biosensor cells, indicating the tau species secreted by tau-overexpressing HEK293 cells was incapable of initiating a sequence of events to seed adjacent cells.

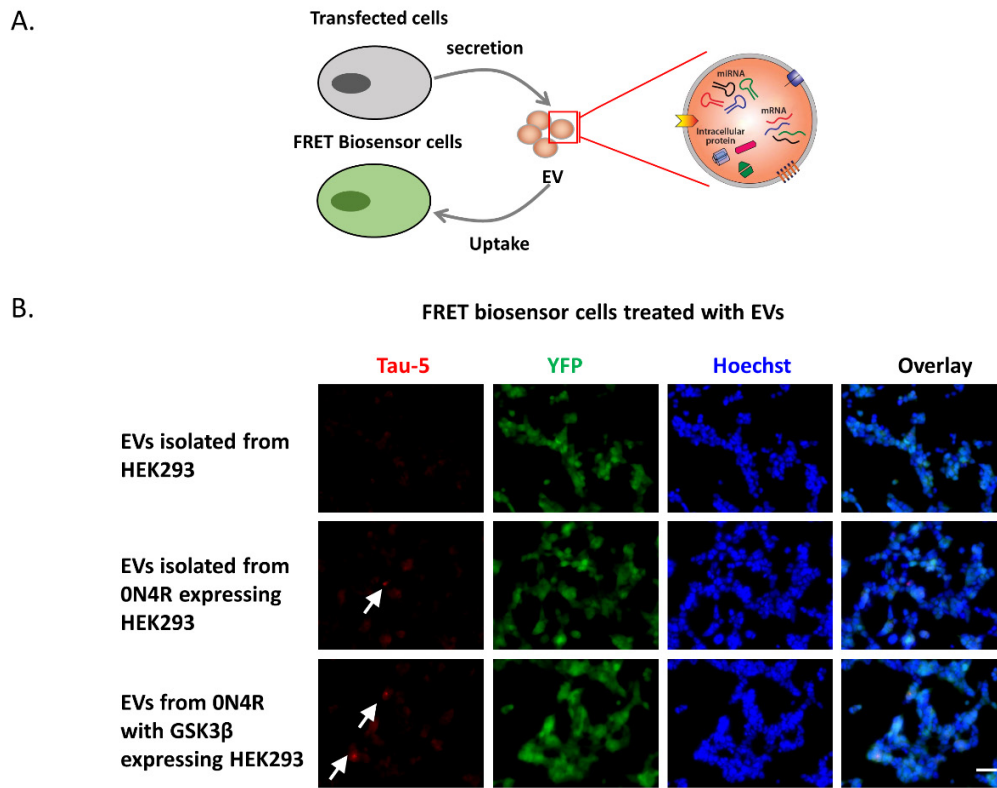


**Figure S4. HEK293 cells with the incubation of exosomes isolated from tau-expressing cells. A.** The schematic illustration of EV-assisted delivery system to investigate transcellular tau propagation. **B.** HEK293 cells were immunostained against Tau-5 (Red) after three days of EV incubation. The scale bar denotes 100  $\mu\text{m}$ .

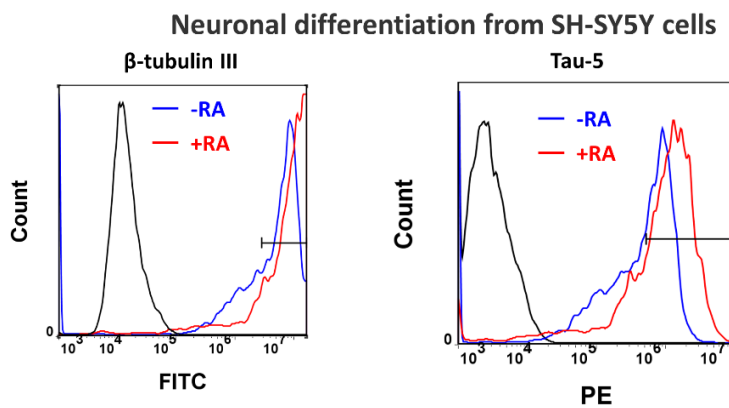


**Figure S5. A higher amount of Tau-5 and  $\beta$ -tubulin III expressions showed in RA-treated SH-SY5Y cells compared to untreated cells, as quantified by flow cytometry.** Representative flow cytometry histograms are shown. Black line: Negative control; blue line: cells without RA; red line: cells differentiated by RA.

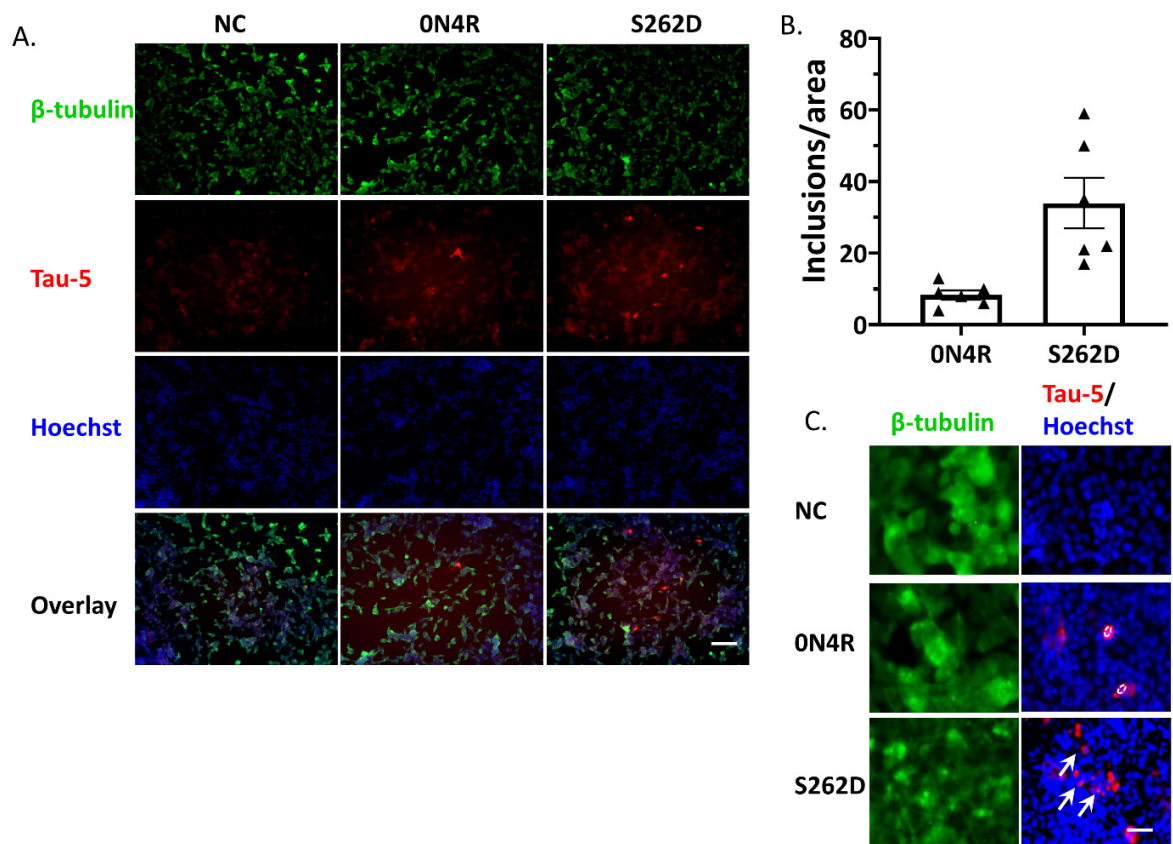


**Figure S6. S262 phosphorylation leads to tau cellular redistribution and tau inclusions in SH-SY5Y cells.** **A.** Representative fluorescent images of the neuronal marker,  $\beta$ -tubulin III (Green), and tau marker, Tau-5 (Red), expressed by SH-SY5Y cells transiently transfected with wild-type ON4R and S262D variant three days following transfection. Negative control (NC): SH-SY5Y cells transfected with pCEP4 plasmid backbone. Scale bar = 100  $\mu$ m. **B.** Quantifications of the number of Tau-5+ pathological inclusions identified in SH-SY5Y cells three days post-transfection with wild-type ON4R and S262D variant. **C.** Co-staining of  $\beta$ -tubulin III and Tau-5 showed an overlap in cellular distribution decreased in SH-SY5Y cells transfected with the S262D variant. Scale bar = 25  $\mu$ m.